

## High Peak Power RF Processing Studies of 3 GHz Niobium Cavities\*

J.Graber, P.Barnes, J.Kirchgessner, D.Moffat, H.Padamsee, D.Rubin, J.Sears, and Q.S.Shu†  
Laboratory of Nuclear Studies, Cornell University  
Ithaca, New York 14853

### Abstract

Field emission is the primary obstacle to improving accelerating gradients in superconducting RF cavities. We are investigating the effects/benefits of High Peak Power (HPP) RF Processing as a means of reducing field emission loading in 3 GHz niobium accelerator cavities. Our test apparatus includes a 3 GHz Klystron capable of delivering RF pulses of up to 200 kW peak power with pulse length up to 2.5 msec at a repetition rate of approximately 1 Hz. The test apparatus has variable coupling such that the input external Q varies between  $10^5$  and  $10^{10}$  without breaking the cavity vacuum. Low power, continuous wave (cw) tests before and after HPP show that HPP is effective in removing emissions which are unaffected by low power RF processing. CW measurements show that field emission reduction is dependent on maximum field reached during HPP. HPP fields of  $E_{\text{peak}} = 70\text{-}72$  MV/m have been attained. These tests showed FE elimination to  $E_{\text{peak}} = 40$  MV/m, and maximum fields of  $E_{\text{peak}} = 50\text{-}55$  MV/m. Temperature mapping is now available. A cavity which showed strong FE loading, and had extensive temperature mapping is now being investigated in an SEM. A nine-cell cavity has been successfully tested, and through HPP, reached  $E_{\text{acc}} = 15$  MV/m, with  $Q_0 = 6.0 \times 10^9$ .

### I. EXPERIMENTAL APPARATUS

This project and its associated hardware were previously described in a paper presented at the 1989 IEEE Particle Accelerator Conference [1].

#### *HPP Test Stand and Klystron*

The HPP test stand was specially designed and constructed for the studies described here. The input RF coupling was designed to provide  $Q_{\text{ext}}$  between  $10^5$  (for HPP Processing) and  $10^{10}$  (for low power cw tests) without breaking the cavity vacuum, thus avoiding surface contamination and associated emission between processing and subsequent cw low power testing.

Diagrams of the HPP test stand and the high power klystron circuit may be found in reference [1].

#### *Cavity Temperature Mapping System*

A recent addition to the HPP test apparatus is a 100 thermometer temperature mapping system. This system is similar to the temperature mapping system which provided significant results in the 1.5 GHz program [2]. It consists of ten boards of ten thermometers each, spaced at  $36^\circ$  intervals around the azimuth of the cavity.

A temperature map (see Figure 5) consists of a ten by ten array of the differences of the outer wall temperature between

RF on and RF Off. Each position on the map corresponds to an individual thermometer. Calibration of the thermometers is done via a calibrated germanium resistance thermometer.

A map can be obtained in approximately 25 seconds when the cavity is operated cw. (The RF-on portion of the mapping takes only 8 seconds.) Temperature maps may also be obtained during HPP pulsing. HPP maps are obtained in about 120 seconds, as the resistors are read one resistor per RF pulse.

### II. EXPERIMENTAL RESULTS

#### *Procedure*

The experimental procedure is generally as follows, with minor alterations on individual tests:

1) Light (2-4 minutes) chemical etch in 1:1:2 BCP, followed by mounting to test stand in clean room environment. (NOTE: Cavities initially had 100 microns removed from their surface via 1:1:1 BCP, prior to equator weld. In light of recent results on hydrogen contamination [3], all subsequent etchings are done with 1:1:2 BCP as opposed to 1:1:1 BCP.)

2) Pre-cool 12-20 hours with liquid nitrogen. Cool to liquid helium temperature, then lower the bath temperature to 1.4-1.5 K.

3) Low power ( $\leq 20$  W) characterization of cavity: obtain a Q vs. E curve, as well as temperature maps at various field levels. Calibrate  $E_{\text{peak}}$  with the output of the transmitted power probe

4) Pulsed HPP processing for 10-60 minutes monitoring field levels in the cavity via transmitted power.

5) Steps 3 and 4 are generally repeated until there is no further gain in low power cavity behavior.

#### *Overall Effect: Reduced Loading of Cavities*

HPP Processing has been found to be effective in raising FE thresholds 60-80% above their initial, chemically polished levels. Figure 1 shows a typical Q vs.  $E_{\text{peak}}$  plot before and after HPP processing.

HPP processing has been shown to increase both the FE threshold and maximum attainable fields. Figures 2 and 3 show increases in FE threshold and peak field respectively. It is interesting to note that the benefits of HPP processing appear to be related to the electric field level reached during the HPP stage, as opposed to the processing power level. Figure 4 shows the relationships between maximum field reached during HPP and subsequent FE threshold and maximum attainable electric field.

We have found the limit on maximum pulsed field during HPP to be 70-72 MV/m ( $H_{\text{peak}} = 1670$  Oe). The limiting effect has been determined (through thermometry and monitoring of the transmitted power) to be thermal breakdown.

\* Supported by N.S.F. with supplementary support from the U.S.-Japan Collaboration.

† Permanent Address: SSC Laboratory, 2550 Beckleymeade ave., Dallas, Texas 75237

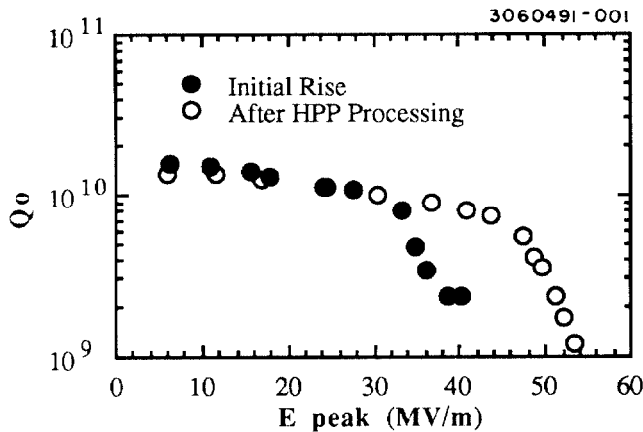


Figure 1. An example of the effect of HPP. 3060491-002

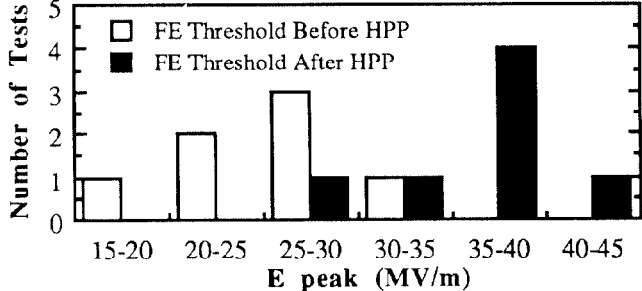


Figure 2. Comparison of the FE Threshold field with and without HPP Processing in 7 tests. 3060491-003

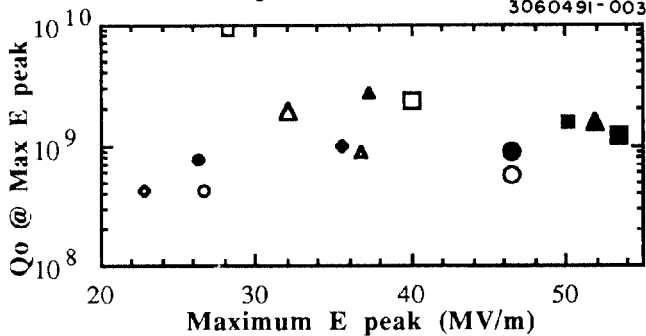


Figure 3. A comparison of maximum attainable peak electric fields (and their associated Qo values), before and after HPP. Open symbols signify prior to HPP, solid symbols signify after HPP. 3060491-004

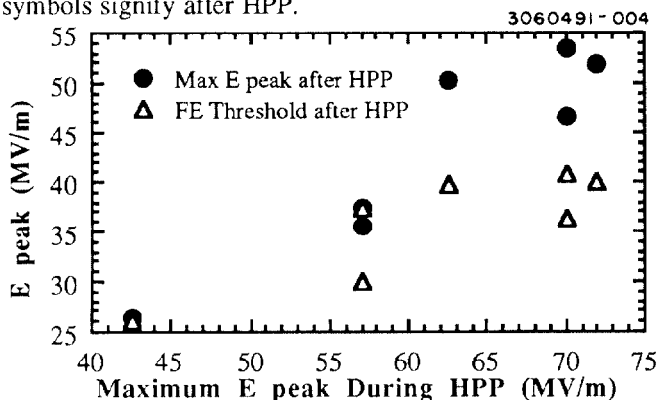


Figure 4. Maximum attainable cw electric field and FE Threshold Field as a function of maximum HPP field. 3060491-005

The cause of this thermal breakdown is a new effect arising from the very high surface magnetic field. More details on this effect at cw fields are presented in another paper [4]. We have labeled this effect Global Thermal Instability (GTI). In GTI, the high magnetic fields in the equator region cause power dissipation at such a rate that the entire equator region heats unstably until  $T_c$  is surpassed and a breakdown occurs.

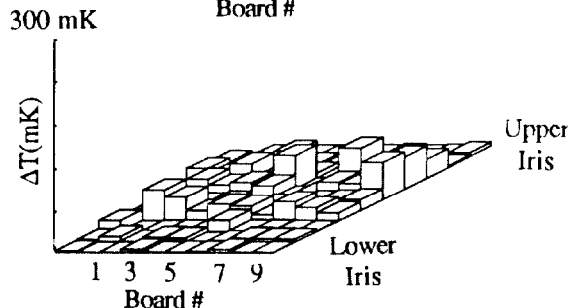
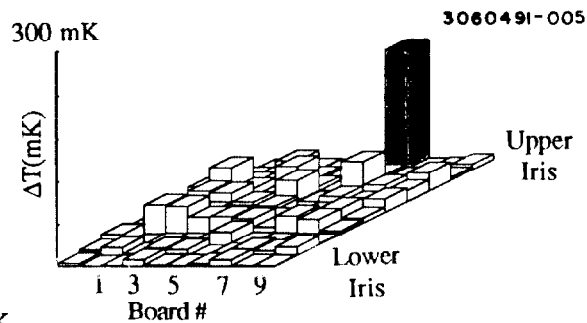


Figure 5. Temperature maps showing the removal of a strong field emission site with HPP Processing. The top map was taken at  $E_{peak} = 48$  MV/m prior to HPP. The bottom map was taken at  $E_{peak} = 49$  MV/m after HPP.

#### Local Effect: Change of $\Delta T$ vs $E$ Behavior

The addition of the temperature mapping system has allowed for a better determination of the local effects of HPP. Temperature maps are made before and after HPP processing. Figure 5 shows an example of the removal of a significant emitter. Often it appears that the effect of HPP is a decrease of emission, as opposed to complete destruction of the emitter. Figure 6 shows the evolution of a  $\Delta T$  vs  $E_{peak}$  behavior of an emitter over the course of several HPP sessions as well as a room temperature cycle.

#### Microscopic Effect: SEM Investigations of Emitters

An ongoing research effort with the "mushroom cavity" [5] has shown that Scanning Electron Microscope (SEM) examination of RF surfaces reveals significant surface features in areas which are subject to field emission. Guided by these findings, a 3 GHz cavity was cut open following a test in which extensive field emission was encountered. The cavity contained sites which were processed through HPP (based on the temperature maps), as well as sites which could not be processed or were partially processed.

Initial investigation of the cavity surface reveals 40 "starburst" features (See Figure 7) similar to those found in the mushroom cavity. This investigation is continuing in an

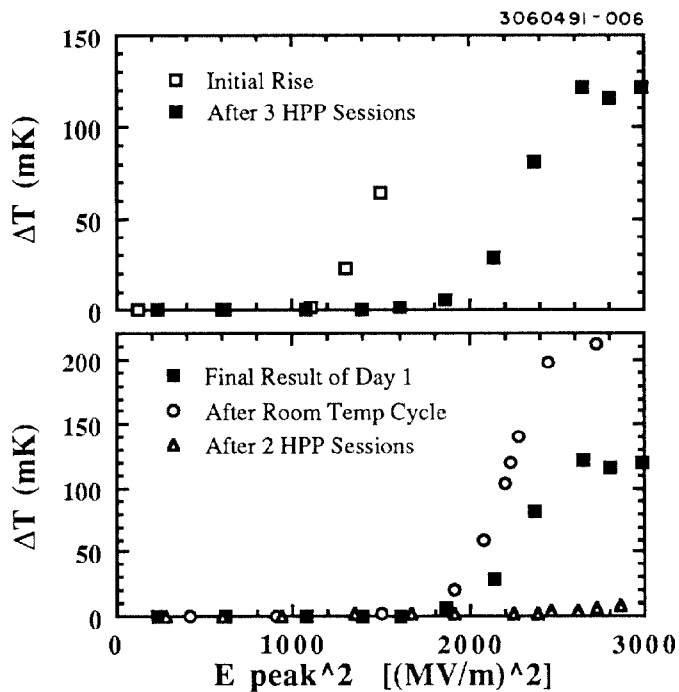


Figure 6. Evolution of  $\Delta T$  vs  $E_{\text{peak}}$  squared over the course of several HPP sessions.

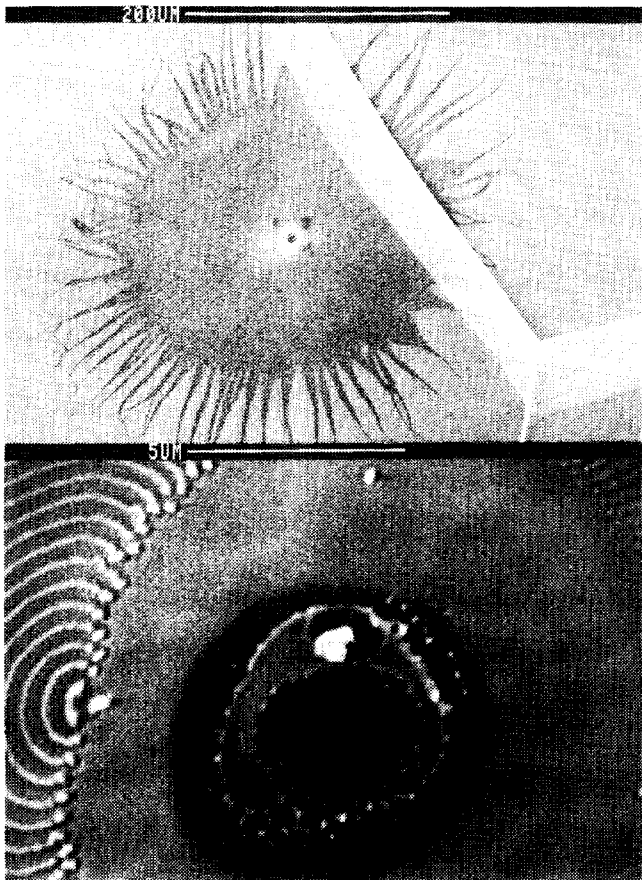


Figure 7. An example of a "starburst" phenomena found on the inside of a 3 GHz cavity in a region known, through thermometry, to have been a strong emission area. The bottom picture is an expanded view of the center of the top picture.

attempt to correlate surface phenomena with HPP results in single-cell cavities.

### Application to Multi-Cell Structures

Accelerators generally use multi-cell cavities as opposed to the single-cell cavities useful for basic research. Therefore it is important to demonstrate the applicability of the HPP technique to multi-cell structures. We have fabricated and performed initial tests on a nine-cell 3 GHz cavity. The results were very encouraging. Prior to HPP, the cavity was limited to  $E_{\text{peak}} = 20$  MV/m with  $Q = 1.3 \times 10^9$ . Following HPP, the cavity reached  $E_{\text{peak}} = 31$  MV/m ( $E_{\text{acc}} = 15$  MV/m) with  $Q = 6.0 \times 10^9$ , a significant reduction in FE loading. Figure 8 shows the  $Q$  vs.  $E_{\text{peak}}$  results for this test. The maximum field was limited by local thermal breakdown. This cavity has now been sent to Wuppertal for tests with heat treatment and to raise the RRR with Ti treatments. Upon completion, it will be retested with HPP to evaluate the effect of improved RRR.

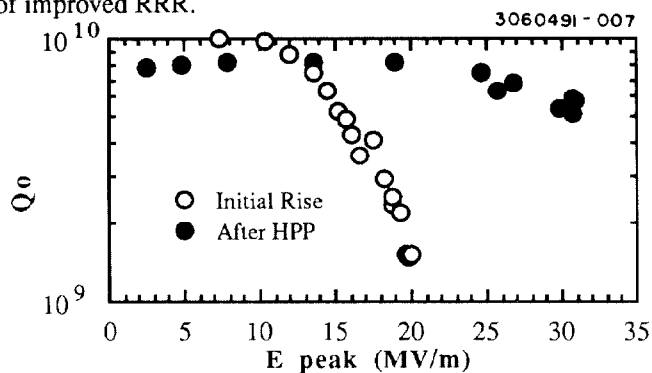


Figure 8.  $Q$  vs  $E_{\text{peak}}$  plot for 9-cell cavity S3C9-1 before and after HPP Processing.

### III. DISCUSSION

HPP Processing has been shown to be an effective means of increasing electric fields in chemically treated cavities to  $E_{\text{peak}} = 50$ -55 MV/m. Benefits increase with field level reachable during processing. The maximum processing surface field of 72 MV/m appears to be limited by a global thermal breakdown. Accordingly the cw maximum field reachable is limited to 55 MV/m. To use this method to reach higher cw fields it will be necessary to either (a) lower the frequency or (b) use a cavity with a reduced  $H_{\text{pk}}/E_{\text{pk}}$  ratio - both in order to avoid the phenomenon of GTI.

### IV. REFERENCES

1. J. Kirchgessner, et.al., *Proceedings of the 1989 IEEE Particle Accelerator Conference*, Chicago, IL, March 20-23, 1989, pp. 482-484.
2. H. Padamsee, et.al., *Proceedings of the 1987 IEEE Particle Accelerator Conference*, Washington, DC, March 16-19, 1987, pp. 1824-1826.
3. D. Moffat, et.al., PTP13, proceedings of this conference.
4. J. Graber, et.al., CLNS 91/1061.
5. D. Moffat, et.al., BGR2, proceedings of this conference.